# Peptide friction in water nanofilm on mica surface*

Zhou Bo(周 波)[a)b)], Xiu Peng(修 鹏)[c)], Wang Chun-Lei(王春雷)[a)], and Fang Hai-Ping(方海平)[a)d)†]

[a)] *Department of Physical Biology and Department of Microscopic Water Dynamics, Shanghai Institute of Applied Physics, Chinese Academy of Sciences, P. O. Box* 800-204, *Shanghai* 201800, *China*

[b)] *Graduate School of the Chinese Academy of Sciences, Beijing* 100190, *China*

[c)] *Bio-X Laboratory, Department of Physics, Zhejiang University, Hangzhou* 310027, *China*

[d)] *Theoretical Physics Center for Science Facilities, Chinese Academy of Sciences,* 19*(B) Yuquan Road, Beijing* 100049, *China*

(Received 17 May 2011; revised manuscript received 22 July 2011)

Peptide frictions in water nanofilms of various thicknesses on a mica surface are studied via molecular dynamics simulations. We find that the forced lateral motion of the peptide exhibits stick-slip behaviour at low water coverage; in contrast, the smooth gliding motion is observed at higher water coverage. The adsorbed peptide can form direct peptide–surface hydrogen bonds as well as indirect peptide–water–surface hydrogen bonds with the substrate. We propose that the stick-slip phenomenon is attributed to the overall effects of direct and indirect hydrogen bonds formed between the surface and the peptide.

**Keywords:** peptide friction, water nanofilm, mica surface, molecular dynamics simulation

**PACS:** 68.35.Af, 81.40.Pq, 68.08.–p, 68.47.Pe **DOI:** 10.1088/1674-1056/21/2/026801

## 1. Introduction

Polymer adsorption, adhesion and friction on inorganic surfaces play a key role in many applications, including surface modification, lubrication, biomineralization and molecular self-assembly.[1−3] In particular, interfacial properties of hybrid interfaces with solid surface, water, organics, and biomolecules are of increasing interest.[4−21] Both atomic force microscope (AFM) experiments and molecular dynamics (MD) simulations have shown that even if the adsorbed polymers exhibit comparable desorption forces, their planar mobility may be drastically different.[22−24] Using MD simulations, Serr *et al.*[22] studied the polypeptide mobility and adhesion in bulk solutions on both hydrophobic and hydrophilic surfaces. They found that forced motion on the hydrophilic surface exhibited stick-slip due to the hydrogen-bond (H-bond) kinetics and the motion was smooth on the hydrophobic surface. Muscovite mica surface is a widely used solid substrate for the study of interfacial phenomena because of its smoothness at the atomic scale. Water adsorbed on the mica surface in ambient conditions exhibits an ice-like structure that epitaxially grows on the substrate and this ordered water has been extensively studied experimentally and theoretically.[25−38] Self-assembly of peptides with charged residues/terminals in bulk solutions was observed on the mica surface,[39,40] however, the highly hydrophobic peptides hardly form epitaxial nanofilaments under the same circumstances. In our previous study, we found an unexpected self-assembly behaviour of the hydrophobic peptides in a water nanofilm condensed on a mica surface,[41] which provided a new insight into some interfacial processes.[42−46] It is expected that polymers interacting with the mica surface at the mica-water interface are different from those interacting with the other surfaces in the absence of interfacial ordered water.

In this study, the forced peptide motions in water nanofilms of various thicknesses on the mica surface are investigated by MD simulations. Both the stick-slip motion and smooth motion are observed at different water coverages. The former motion corresponds to a lateral friction force with pronounced loading-release cycles, whereas the latter one corresponds to a rather constant force. The H-bond kinetics resulting from direct peptide–surface H bonds and indirect peptide–water–surface H bonds, as well as from the peptide main chain and side chains, is discussed. We

*Project supported by the National Natural Science Foundation of China (Grant No. 10825520), the National Basic Research Program of China (Grant No. 2007CB936000), and the National Science Foundation for Post-Doctoral Scientists of China (Grant No. 20100480645).

†Corresponding author. E-mail: fanghaiping@sinap.ac.cn

© 2012 Chinese Physical Society and IOP Publishing Ltd

propose that the overall effects of the direct and indirect H bonds formed between the surface and the peptide dominate the stick-slip behaviour observed at low water coverage.

## 2. Model and methods

The $2M_1$-muscovite mica has a structure of 2:1 layered dioctahedral (hydroxy-) aluminosilicate with formula unit $KAl_2(Si_3Al)O_{10}(OH)_2$. A layer of mica surface consists of one octahedral aluminum sheet sandwiched between two tetrahedral silicon sheets which expose the basal oxygen atoms of the six-member (Si, Al) rings, and can be built by cleaving the muscovite along the (001) plane in the middle of interlayer space. Substituting Si by Al in the tetrahedral sheets with a ratio of Al/Si = 1/3 results in a net negative surface charge which is balanced by potassium counterions.

In this study, the model decapeptide (Ace-(Val-Asn)$_5$-NMe) is composed of alternating valine and asparagine residues and its N-terminus and C-terminus are protected by acetyl and methylamide groups, respectively. Water shells with the number of water molecules $N$ = 0, 100, 200, 300, 400, 500, 600, 700, and 900 were placed around the peptide, resulting in nine different systems. A monolayer coverage of water on the mica surface in the absence of peptide corresponds to $N$ = 288 in the present work.[26,28,32] The initial configuration of simulation box is schematically shown in Fig. 1 (drawn with VMD 1.9[47]). The minimal distance between the outmost water shell and the average position of surface basal oxygen atoms was set to be approximately 0.7 nm in each system. The unit cell parameters for bulk mica were taken from the high-resolution X-ray reflectivity study,[48] and all tetrahedral Al atoms were arranged in an ordered fashion as indicated in Ref. [32]. The mica surface consists of 12 × 4 unit cells and the final rectangular simulation box for each system had $x$, $y$ and $z$ dimensions of 6.20 nm × 3.58 nm × 20 nm, which included a free space of at least 15 nm in the $z$ direction. A repulsive potential wall was placed at $z$ = 14 nm in each simulation box to prevent vaporized water molecules from trapping by the periodic image of mica surface.

All MD simulations were performed using the GROMACS program package.[49] The CLAYFF[50] force field and the SPC[51] water model were used to simulate the mica surface and water, respectively. The CLAYFF has been used to well reproduce the experimental crystal structure for mica as well as to study the mica-water interface via MD simulations.[32] Parameters for the peptide were derived from the Amber ff99SB-ILDN[52] force field. The Lorentz–Berthelot mixing rules[53] were used for the mixture parameters: $\varepsilon_{ij} = (\varepsilon_{ii}\varepsilon_{jj})^{1/2}$ and $\sigma_{ij} = (\sigma_{ii} + \sigma_{jj})/2$, where, $\varepsilon_{ii}$ and $\sigma_{ii}$ are the parameters of atom $i$ for interaction energy and molecular diameter, respectively. The particle mesh Ewald (PME) method with a correction term for slab geometry[54] was used to treat long-range electrostatic interactions, whereas the van der Waals interactions were treated with a cutoff distance of 1.0 nm. The temperature and pressure were controlled using velocity rescaling thermostat[55] and Parrinello–Rahman pressure coupling scheme,[56] respectively. All bonds connecting hydrogen atoms were constrained using SETTLE[57] for the water molecules and P-LINCS[49] for the peptide and the mica surface. Periodic boundary conditions were used in the three directions. A time step of 2 fs was used and the data were collected every 1 ps.

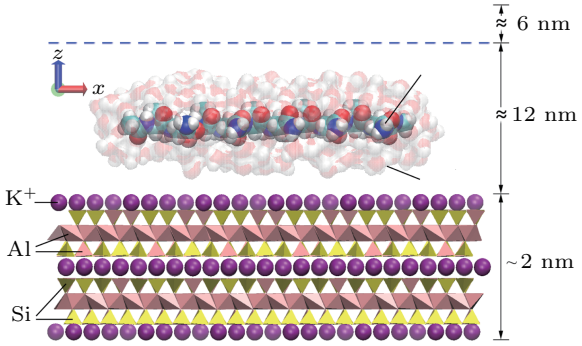



**Fig. 1.** (colour online) Schematic representation (side view along the $x$ direction) of the initial configuration of simulation box. O atoms are depicted in red, N in blue, C in cyan, H in white and $K^+$ ions in purple. Water molecules are represented by surface rendering method. The triangular polyhedra contain Si (yellow) and aluminum (pink) in the centre and the other polyhedra are Al octahedra. The position of the repulsive potential wall is depicted as blue dashed line.

In order to determine the $x$ and the $y$ supercell dimensions for the mica surface, preliminary calculations consisted sequentially of energy minimization, 100-ps MD runs at constant volume and constant temperature (NVT) of 300 K and 4-ns MD runs at constant pressure and temperature (NPT) of 1 bar (1 bar=$10^5$ Pa) and 300 K, respectively. The last 2 ns was used to determine the final supercell dimensions. With the predetermined box parameters, further relaxations of each system were achieved in three stages. Initially, the mica surface was held rigid and the energy of the system was minimized. This was followed by 100-ps MD runs in the NVT ensemble to ensure

the complete adsorption of the peptide–water mixture on the surface. Then the system was equilibrated for 50 ps with all atoms of the system being free to relax.

The next 30-ns production runs started with these optimized configurations and the total momentum was set to be zero. The terminal NMe residue moved along the $x$ axis at a velocity of 0.5 m/s by using the pull code with a spring constant of 500 kJ·mol$^{-1}$·nm$^{-2}$. The pull code implemented in GROMACS has been successfully used to mimic the AFM experiments in previous MD studies.[16,22,58,59] Error estimates were determined by block averaging.[60]

## 3. Results and discussion

It has been demonstrated that the friction coefficient of a polymer molecule adsorbed on a surface is not only dependent on the peptide adsorption force, but also related to the surface potential corrugations.[22–24] Figure 2 clearly shows that the number of water molecules on the surface, $N$, drastically influences the friction and the adsorption of the peptide. The average lateral friction force is about $\overline{F}_x \approx 922.0$ pN at the dry surface ($N = 0$) and then decreases with $N$ increasing and finally reaches $\overline{F}_x \approx 4.5$ pN when 900 water molecules are present in the system, which is approximately 200-fold reduced compared with the mean friction force at $N = 0$. It should be pointed out that the mean friction force decreases very gradually at $100 \leq N \leq 200$ and at $300 \leq N \leq 500$. The average distance $Z$ between the $C_\alpha$ atoms of the peptide and surface basal oxygen atoms increases monotonically with the increase

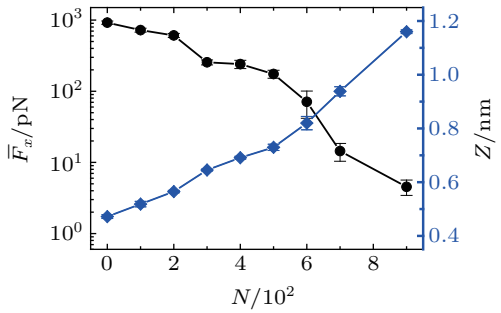



**Fig. 2.** (colour online) Average lateral friction force $\overline{F}_x$ (black circles) of the peptide together with the corresponding average distance $Z$ (blue diamonds) between the $C_\alpha$ atoms of the peptide and surface basal oxygen atoms, versus the number $N$ of water molecules on the mica surface.

of the number of water molecules on the surface, indicating that the peptide has an affinity for the air–water interface and the peptide adsorption force on the mica surface is weakened as more water molecules are present on the surface. In the previous study, Whitehouse *et al.*[40] found that the spontaneous formation of $\beta$-sheet tapes at the mica surface in aqueous solution was unable to be imaged by AFM, unless the peptide/binding energy was raised by using a solvent mixture of 10% water in 2-propanol (v/v). Engin *et al.*[61] studied the partitioning of amphiphilic peptides at the air–water interface via MD simulations and they concluded that the dehydration of hydrophobic peptide side chains dominates the free energy of transferring the amphiphilic peptides from bulk water to the air–water interface. We note that these results are in agreement with ours.

A detailed analysis of the lateral friction force with two different numbers of water molecules is shown in Fig. 3 for comparison. The time evolution of the lateral displacement in the system with 200 water molecules displays a distinct stick-slip behaviour, whereas an almost smooth gliding motion is observed for the peptide in the system with 700 water molecules (see Fig. 3(a)). From Fig. 3(b) commensurate with the

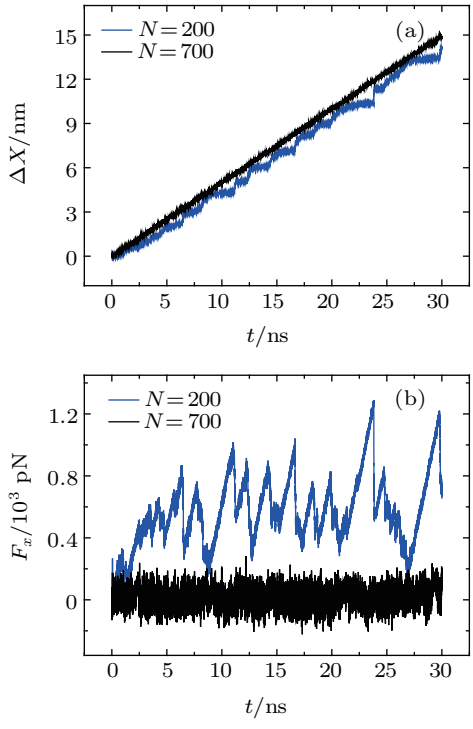



**Fig. 3.** (colour online) (a) Lateral displacement $\Delta X$ and (b) lateral friction force $F_x$ of the peptide, each as a function of simulation time $t$, for the system containing $N = 200$ (blue) and $N = 700$ (black) water molecules, respectively.

lateral displacement, we observe many loading-release cycles with force spikes up to $F_x \approx 1300$ pN in the system with 200 water molecules. On the other hand, the lateral friction force fluctuates around its mean value

of 14.4 pN in the system with 700 water molecules. It should be pointed out that the latter motion is similar to the polypeptide friction on a hydrophobic surface.[22] We also note that there is only one or two water layers sandwiched between the peptide and the mica surface in the system with 200 water molecules (see Fig. 2) and the restricted lateral translations of these interfacial water molecules[32] may influence the lateral friction of the peptide.

In the presence of water adsorbed on the surface, the peptide binds to the surface with specific functional groups, while the rest is mainly immersed in the water. It is expected that the adsorption process of the dissolved or partially dissolved peptide in water nanofilm will be in competition with the interfacial water molecules on the surface. There are two probable manners for the peptide to interact with the surface: either through the formation of direct peptide–surface H bonds or through the formation of indirect peptide–water–surface H bonds. Moreover, both the peptide main chain and the polar side chains could contribute to these two types of H bonds. Figure 4 shows the average number of H bonds $\overline{n}_{\rm HB}$ as a function of the number of water molecules on the mica surface. The direct and the indirect H bonds together with their sum, as well as the decomposed contributions from the main chain and side chains, are considered. The geometrical criterion was used here to define the existence of an H bond when the O···O distance is less than 0.35 nm and the angle H–O···O is less than 30°.[62] As shown in Fig. 4(a), the direct H bonds formed between the surface and the peptide are attributed mainly to the side chains. The peptide main chain hardly forms any H bond with the surface in the presence of water. The direct $\overline{n}_{\rm HB}$ contributed from the side chains gradually decreases to zero at $N > 400$. This can be explained as follows. The optimal distance between the Asn–$NH_2$ group and the corresponding $C_\alpha$ atom is approximately 0.37 nm. At $N = 500$, the average distance between the peptide $C_\alpha$ atoms and surface basal oxygen atoms is about 0.73 nm. Thus, the mean minimal distance between Asn–$NH_2$ groups and surface basal oxygen atoms is obtained to be 0.36 nm, which is slightly beyond the intermolecular O···N cutoff distance when one H bond is estimated to form. It should be pointed out that the direct $\overline{n}_{\rm HB}$ contributed from the side chains exhibits an abrupt decrease from $N = 200$ to $N = 300$, which indicates that the hydration layer shields the surface.

In Fig. 4(b), we show that the indirect H bonds formed between the surface and the peptide main chain almost vanish at $N > 500$, which is attributed to the increased thickness of the sandwiched water layers between the peptide and the mica surface (see Fig. 2). The indirect $\overline{n}_{\rm HB}$ contributed from the side chains increases very gradually from $N = 100$ to $N = 500$, which is accompanied by the loss of direct

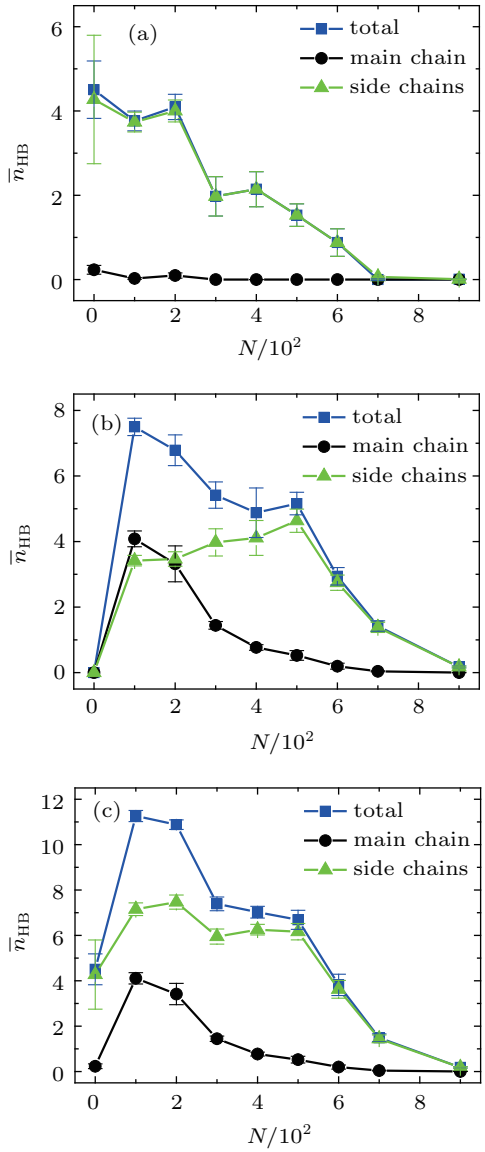



**Fig. 4.** (colour online) Average number of H bonds $\overline{n}_{\rm HB}$ as a function of the number $N$ of water molecules on the mica surface. (a) Direct and (b) indirect H bonds and (c) their sum are shown separately. Total (blue squares) number of H bonds is decomposed into the sum of the number of H bonds contributed from the peptide main chain (black circles) and that from the side chains (green triangles).

H bonds formed between the surface and the peptide side chains (see Fig. 4(a)). As a result, we observe from Fig. 4(c) that the peptide side chains have a lower propensity to form H bonds with the surface through direct and indirect interactions as more water molecules are present on the surface. The overall $\overline{n}_{\rm HB}$ formed between the surface and the peptide, decreasing with the number of water molecules on the

substrate increasing, slowly varies at $100 \leq N \leq 200$ and at $300 \leq N \leq 500$. We note that these two regions exactly coincide with the regions where $\overline{F}_x$ varies gradually as observed in Fig. 2, suggesting that the overall effects of direct and indirect H bonds formed between the surface and the peptide determine the lateral friction force of the peptide.

As mentioned above, the lateral displacement of the peptide pulled along the surface correlates to the lateral friction force. In other words, the lateral friction force with distinct loading-release cycles indicates the occurrence of a stick-slip motion and *vice versa*. To reveal the relationship between the lateral motion of the peptide and the peptide−surface interactions, we take the system with 200 water molecules for example. The time evolutions of the number of direct and indirect H bonds, and their sum, as well as the time evolutions of lateral displacement of the peptide, are shown in Fig. 5. At $t = 16$ ns, a breakage of the indirect H bonds occurs (Fig. 5(b)), while the direct H

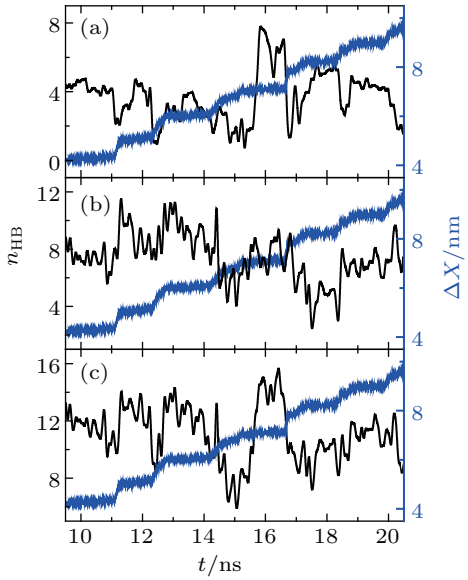



**Fig. 5.** (colour online) Number of H bonds $\overline{n}_{\rm HB}$ (black, smoothed over 50 ps) with respect to simulation time $t$ and the corresponding lateral displacement $\Delta X$ (blue), for system containing 200 water molecules. (a) Direct and (b) indirect H bonds, and (c) their sum are shown separately. Only the results for $9.5 \leq t \leq 20.5$ ns are shown for clarity.

bonds are still maintained (Fig. 5(a)). Subsequently, a breakage of the direct H bonds appears, whereas a reformation of the indirect H bonds is observed. At $t \approx 16.6$ ns, the number of direct H bonds and that of indirect H bonds decrease simultaneously, which is accompanied by a slippage event. Note that the breakages of the overall H bonds including both direct and indirect contributions, coincide well with the slippage events (Fig. 5(c)). This suggests that the overall effects of direct and indirect H bonds formed between the surface and the peptide dominate the stick-slip behaviour of the peptide pulled along the mica surface.

## 4. Conclusions

Peptide adsorption and friction on the mica surface are strongly associated with the thickness of the water nanofilm adsorbed on the substrate. As a result of the weak adsorption force on the substrate and the affinity for the air–water interface, the average lateral friction force of the peptide on the dry surface is about two orders of magnitude larger than that with a water nanofilm of $\sim$ 1-nm thickness on the surface. The forced lateral motion of the peptide exhibits a stick-slip behaviour at low water coverage; in contrast, the peptide motion is smooth at higher water coverage.

The peptide can form direct peptide–surface H bonds as well as indirect peptide–water–surface H bonds with the substrate. We find that the peptide main chain hardly forms direct hydrogen bond with the mica surface. Thus, we expect that the peptide composed of only hydrophobic amino acids, interacts with the substrate through the formation of indirect H bonds in the presence of the water nanofilms. These indirect H bonds could be responsible for the "epitaxial" self-assembly behaviours of the hydrophobic peptides in ambient water nanofilms on the mica surface.[41] After careful analysis of a 11-ns trajectory, we conclude that the overall effects of direct and indirect H bonds formed between the surface and the peptide dominate the stick-slip behaviour observed at low water coverage.

## Acknowledgment

We thank Dr. Ren Xiu-Ping for reading the manuscript.

## References

[1] Harding J H, Duffy D M, Sushko M L, Rodger P M, Quigley D and Elliott J A 2008 *Chem. Rev.* **108** 4823
[2] Gray J J 2004 *Curr. Opin. Struct. Biol.* **14** 110
[3] Netz R R and Andelman D 2003 *Phys. Rep.* **380** 1
[4] Monti S, Alderighi M, Duce C, Solaro R and Tine M R 2009 *J. Phys. Chem.* C **113** 2433
[5] Nonella M and Seeger S 2010 *Chem. Phys.* **378** 73
[6] Sheng Y B, Wang W and Chen P 2010 *Protein Sci.* **19** 1639

[7] Calzolari A, Cicero G, Cavazzoni C, Di Felice R, Catellani A and Corni S 2010 *J. Am. Chem. Soc.* **132** 4790

[8] Pirzer T and Hugel T 2009 *Chem. Phys. Chem.* **10** 2795

[9] Geisler M, Horinek D and Hugel T 2009 *Macromolecules* **42** 9338

[10] Cole D J, Payne M C and Ciacchi L C 2009 *Phys. Chem. Chem. Phys.* **11** 11395

[11] Truhlar D G 2008 *J. Am. Chem. Soc.* **130** 16824

[12] Horinek D, Serr A, Geisler M, Pirzer T, Slotta U, Lud S Q, Garrido J A, Scheibel T, Hugel T and Netz R R 2008 *Proc. Natl. Acad. Sci. USA* **105** 2842

[13] Desai T G, Keblinski P, Kumar S K and Granick S 2007 *Phys. Rev. Lett.* **98** 218301

[14] Magdans U, Torrelles X, Angermund K, Gies H and Rius J 2007 *Langmuir* **23** 4999

[15] Heinz H, Koerner H anderson K L, Vaia R A and Farmer B L 2005 *Chem. Mater.* **17** 5658

[16] Xiu P, Zhou B, Qi W P, Lu H J, Tu Y S and Fang H P 2009 *J. Am. Chem. Soc.* **131** 2840

[17] Zuo G H, Huang Q, Wei G H, Zhou R H and Fang H P 2010 *ACS Nano* **4** 7508

[18] Geisler M, Netz R R and Hugel T 2010 *Angew. Chem. Int. Ed.* **49** 4730

[19] Wang C L, Li Z X, Li J Y, Xiu P, Hu J and Fang H P 2008 *Chin. Phys.* B **17** 2646

[20] Zhang X J, Dong Y K, Liu B H and Schaefer J A 2009 *Chin. Phys.* B **18** 231

[21] Zhou X Y and Lu H J 2007 *Chin. Phys.* **16** 335

[22] Serr A, Horinek D and Netz R R 2008 *J. Am. Chem. Soc.* **130** 12408

[23] Kuhner F, Erdmann M, Sonnenberg L, Serr A, Morfill J and Gaub H E 2006 *Langmuir* **22** 11180

[24] Serr A, Sendner C, Muller F, Einert T R and Netz R R 2010 *Europhys. Lett.* **92** 38002

[25] Hu J, Xiao X D, Ogletree D F and Salmeron M 1995 *Science* **268** 267

[26] Odelius M, Bernasconi M and Parrinello M 1997 *Phys. Rev. Lett.* **78** 2855

[27] Miranda P B, Xu L, Shen Y R and Salmeron M 1998 *Phys. Rev. Lett.* **81** 5876

[28] Cantrell W C and Ewing G E 2001 *J. Phys. Chem.* B **105** 5434

[29] Cheng L, Fenter P, Nagy K L, Schlegel M L and Sturchio N C 2001 *Phys. Rev. Lett.* **87** 156103

[30] Park S H and Sposito G 2002 *Phys. Rev. Lett.* **89** 85501

[31] Spagnoli C, Loos K, Ulman A and Cowman M K 2003 *J. Am. Chem. Soc.* **125** 7124

[32] Wang J W, Kalinichev A G, Kirkpatrick R J and Cygan R T 2005 *J. Phys. Chem.* B **109** 15893

[33] Park C, Fenter P A, Nagy K L and Sturchio N C 2006 *Phys. Rev. Lett.* **97** 016101

[34] Meleshyn A 2008 *J. Phys. Chem.* C **112** 14495

[35] Malani A and Ayappa K G 2009 *J. Phys. Chem.* B **113** 1058

[36] Xu K, Cao P G and Heath J R 2010 *Science* **329** 1188

[37] Sakuma H and Kawamura K 2009 *Geochim. Cosmochim. Acta* **73** 4100

[38] Leng Y and Cummings P T 2005 *Phys. Rev. Lett.* **94** 26101

[39] Zhang F, Du H N, Zhang Z X, Ji L N, Li H T, Tang L, Wang H B, Fan C H, Xu H J, Zhang Y, Hu J, Hu H Y and He J H 2006 *Angew. Chem. Int. Ed.* **45** 3611

[40] Whitehouse C, Fang J Y, Aggeli A, Bell M, Brydson R, Fishwick C W G, Henderson J R, Knobler C M, Owens R W, Thomson N H, Smith D A and Boden N 2005 *Angew. Chem. Int. Ed.* **44** 1965

[41] Li H, Zhang F, Zhang Y, Ye M, Zhou B, Tang Y Z, Yang H J, Xie M Y, Chen S F, He J H, Fang H P and Hu J 2009 *J. Phys. Chem.* B **113** 8795

[42] Ye M, Zhang Y, Li H, Xie M Y and Hu J 2010 *J. Phys. Chem.* B **114** 15759

[43] Ye M, Li B, Zhang Y, Li H, Wang X Y and Hu J 2011 *J. Phys. Chem.* B **115** 2754

[44] Billingsley D J, Kirkham J, Bonass W A and Thomson N H 2010 *Phys. Chem. Chem. Phys.* **12** 14727

[45] Wang C L, Lu H J, Wang Z G, Xiu P, Zhou B, Zuo G H, Wan R Z, Hu J Z and Fang H P 2009 *Phys. Rev. Lett.* **103** 137801

[46] Wang C L, Zhou B, Xiu P and Fang H P 2011 *J. Phys. Chem.* C **115** 3018

[47] Humphrey W, Dalke A and Schulten K 1996 *J. Mol. Graphics* **14** 33

[48] Schlegel M L, Nagy K L, Fenter P, Cheng L, Sturchio N C and Jacobsen S D 2006 *Geochim. Cosmochim. Acta* **70** 3549

[49] Hess B, Kutzner C, van der Spoel D and Lindahl E 2008 *J. Chem. Theor. Comput.* **4** 435

[50] Cygan R T, Liang J J and Kalinichev A G 2004 *J. Phys. Chem.* B **108** 1255

[51] Berendsen H J C, Postma J P M, van Gunsteren W F and Hermans J 1981 *Intermolecular Forces* (Dordrecht: D. Reidel) pp. 331–342

[52] Lindorff-Larsen K, Piana S, Palmo K, Maragakis P, Klepeis J L, Dror R O and Shaw D E 2010 *Proteins: Struct. Funct. Bioinform.* **78** 1950

[53] Allen M P and Tildesley D J 1987 *Computer Simulation of Liquids* (New York: Oxford University Press) p. 21

[54] In-Chul Y and Max L B 1999 *J. Chem. Phys.* **111** 3155

[55] Bussi G, Donadio D and Parrinello M 2007 *J. Chem. Phys.* **126** 014101

[56] Parrinello M and Rahman A 1981 *J. Appl. Phys.* **52** 7182

[57] Miyamoto S and Kollman P A 1992 *J. Comput. Chem.* **13** 952

[58] Qi W, Lei X and Fang H 2010 *ChemPhysChem* **11** 2146

[59] Argyris D, Ashby P D and Striolo A 2011 *ACS Nano* **5** 2215

[60] Hess B 2002 *J. Chem. Phys.* **116** 209

[61] Engin O, Villa A, Sayar M and Hess B 2010 *J. Phys. Chem.* B **114** 11093

[62] Luzar A and Chandler D 1996 *Nature* **379** 55